Article ID: 1003－6326(2003)04－0926－04

Phase structure and electrochemical properties of melt-spinning alloy Zr(MnVNi)$_{2.4}$①

ZHANG Shu-kai(张书凯)[1], SHU Kang-ying(舒康颖)[1], LEI Yong-quan(雷永泉)[2], LÜ Guang-lei(吕光烈)[3], WANG Qi-dong(王启东)[2]

(1. Department of Materials Science and Engineering, Zhejiang University, Hangzhou 310027, China;
2. Ningbo Yunsheng Magnetic Material and Engineering Research Institute, Yunsheng Group, Ningbo 315041, China;
3. Central Laboratory, Zhejiang University, Hangzhou 310028, China)

Abstract: Zr($Mn_{0.2}V_{0.2}Ni_{0.6}$)$_{2.4}$ alloy was prepared by using both arc-melting and melt-spinning processes. The XRD results indicate that the as-cast alloy contains two Laves phases, C14 (15.45%) and C15 (76.48%), and the non-Laves phase Zr_7M_{10} (8.07%, M presents Ni, Mn, V). Meanwhile the melt-spun alloy only has the C14 (27.67%) and C15 (69.43%) Laves phases. The electrochemical test indicates that the melt-spun alloy has much better cycling stability (S_{500}= 90.8%), higher discharge capacity (C_{max}= 347.5 mA·h·g^{-1}) than those of as-cast alloy (S_{500}= 80.9%, C_{max}= 340.8 mA·h·g^{-1}), although its activation property and high-rate dischargeability decrease somewhat. The different electrochemical properties between the melt-spun and as-cast alloys are resulted from the different phase composition, phase abundance and microstructure.

Key words: AB_2 type alloys; melt-spun; over-stoichiometry; electrochemical properties; microstructure

CLC number: TG 132 **Document code:** A

1 INTRODUCTION

It is well known that Zr-based AB_2 Laves phase alloy electrodes have higher discharge capacity and much better cycling stability than that of AB_5 alloys although it is expensive compared to AB_5 alloys. How to further improve the ratio of properties and price of AB_2 alloys has been drawing the interest of many investigators. Some investigations revealed that over-stoichiometric AB_5 type alloys had better charge-discharge cycling stability than stoichiometric alloys[1-5], and some over-stoichiometric AB_2 type alloys showed higher discharge capacity[6, 7]. Meanwhile in resent years, the rapid solidification method has been applied for AB_5 and AB_2 electrode alloys successfully[8-11]. Higashiyama's investigation showed that melt-spinning over-stoichiometric AB_5 type alloys could improve the cycling stability obviously without lowering the discharge capacity obviously[12], but this kind of work has not been done for Zr-based Laves phase alloys yet. In this paper, the effect of rapid solidification method (melt-spinning) on the phase compositions and electrochemical properties of Zr($Mn_{0.2}V_{0.2}Ni_{0.6}$)$_{2.4}$ alloy is investigated.

2 EXPERIMENTAL

Zr($Mn_{0.2}V_{0.2}Ni_{0.6}$)$_{2.4}$ alloy samples, where Zr, Ni, V and Mn have a purity higher than 99.9%, were prepared by arc melting on water-cooled copper hearth under an argon atmosphere, and remelted four times to ensure good homogeneity. The cooling rate of the alloy in the copper crucible was about 100 K·s^{-1}. Part of the alloy was remelted and prepared by melt-spinning method, and the cooling rate was 10 m/s.

The samples were crushed and ground into powder of less than 40 μm and used for electrochemical measurements and X-ray diffraction (XRD) measurements. The electrode pellets (10 mm in diameter) were prepared by cold pressing the mixtures of milled alloy powder (about 100 mg) and powdered electrolytic copper (44 μm) in a mass ratio of 1∶2 into copper holders to form pores. Electrochemical charge-discharge tests were carried out in a tri-electrode electrolysis cell. The discharge capacities of hydride electrodes were determined by galvanostatic method. In electrochemical cycling measurements, the electrodes were charged at a current density of 100 mA·g^{-1} and discharged at 50 mA·g^{-1}. The cut-off potential was set to －0.6V vs Hg|HgO, with the same procedure as reported in Ref. [11].

The phase structure of the samples was determined by XRD analysis using a X-ray diffractometer of Rikagu D/Max-313 with Cu K_α radiation. The

① **Foundation item:** Project(863-715-004-0060) supported by the National Advanced Materials Committee of China
Received date: 2002－05－17; **Accepted date:** 2002－08－28
Correspondence: ZHANG shu-kai, Senior Engineer, PhD candidate; Tel: +86-574-87833987; E-mail: zhangsk@yahoo.com

continuous scanning speed was 4 °/min, and the 2 θ range was 20° - 80°. And the results were analyzed with Rietveld method [11].

The microstructure of the samples was investigated by using scanning electron microscope (SEM) Philips-XL30.

3 RESULTS AND DISCUSSION

Fig. 1 shows the activation process and discharge capacity of as-cast alloys $Zr(Mn_{0.2}V_{0.2}Ni_{0.6})_x$ (x = 2, 2.4). It can be seen that the over-stoichiometric alloy $Zr(Mn_{0.2}V_{0.2}Ni_{0.6})_{2.4}$ has shorter activation process and higher charge-discharge capacity (C_{max} = 332.8 mAh·g^{-1} for x = 2 and C_{max} = 340.8 mAh·g^{-1} for x = 2.4). Fig. 2 shows the electrochemical cycling stability of the two alloys. After 500 charge-discharge cycles, the capacity attenuation rate (S_{500}) of x = 2.4 alloy is 80.9%, and that of x = 2.0 alloy is 75.3%. Because of its relatively better electrochemical properties, we select the alloy $Zr(Mn_{0.2}V_{0.2}Ni_{0.6})_{2.4}$ as the mother alloy.

Fig. 3 shows the XRD patterns of the as-cast and melt-spun $Zr(Mn_{0.2}V_{0.2}Ni_{0.6})_{2.4}$ alloys. Fig. 3(a) presents the peaks of the as-cast alloy which has the C14, C15 Laves phase and Zr_7M_{10} phase. The pattern of melt-spun alloy (shown in Fig. 3(b)) only has the peaks of C14 and C15 Laves phases. The data of XRD are analyzed with Rietveld method, and summarized in Table 1. From Table 1 it can be found that rapid solidification process decreases the C15 phase abundance from 76.48% of as-cast alloy to 69.43% of melt-spun alloy, meanwhile the as-cast alloy contains 8.07% Zr_7M_{10} non-Laves phase, and for the melt-spun alloy, the non-Laves phase disappears. After the melt-spinning process, the lattices constant of C15 phase is decreased from 0.704 78 nm to 0.704 64 nm, and the lattice constants a and c of C14 phase are decreased from 0.499 94, 0.815 65 to 0.497 82, 0.813 75, respectively. These results reveal that rapid solidification process changes the arrangement of atoms in the alloys, and hinders the formation of the non-Laves phase.

Fig. 4 shows the SEM morphology of as-cast and melt-spun $Zr(Mn_{0.2}V_{0.2}Ni_{0.6})_{2.4}$ alloys. The as-cast alloy has very coarse dendritic structure (Fig. 4 (a)) and the melt-spun alloy has a mixed structure of fine dendrites and columnar grains (Fig. 4 (b)).

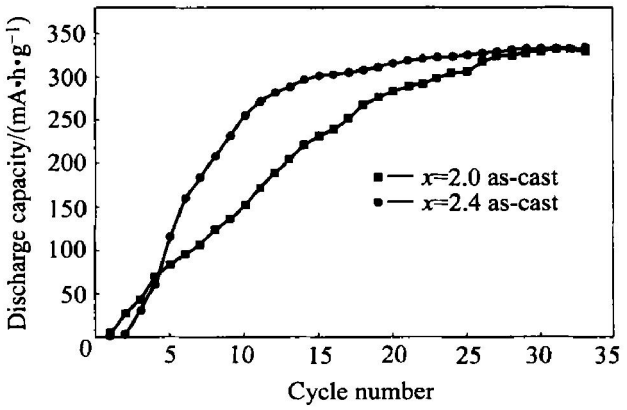

Fig. 1 Activation process of $Zr(Mn_{0.2}V_{0.2}Ni_{0.6})_x$ alloy for x = 2.0 and x = 2.4

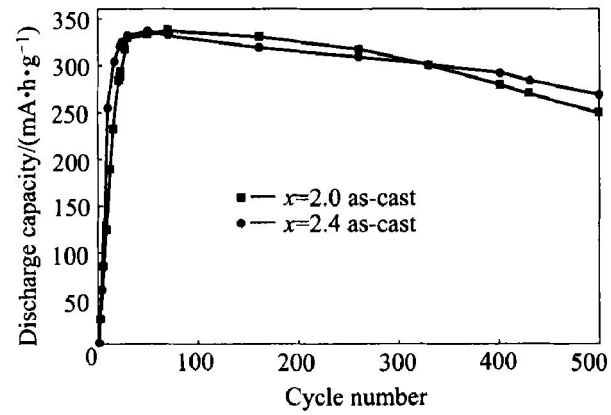

Fig. 2 Cycling stability of $Zr(Mn_{0.2}V_{0.2}Ni_{0.6})_x$ alloy for x = 2.0 and x = 2.4

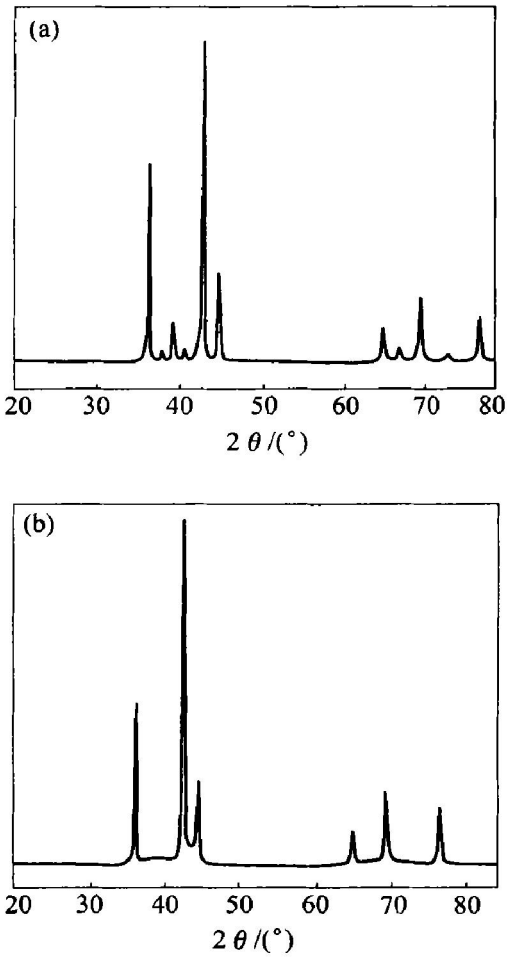

Fig. 3 XRD patterns of two types of alloys Zr(MnVNi)$_{2.4}$
(a) —As-cast; (b) —Melt-spun

Table 1 Lattice parameter of alloys of melt-spun and arc-melted $Zr(Mn_{0.2}V_{0.2}Ni_{0.6})_{2.4}$

Alloy	Phase and composition		Lattice constant			
	Phase	Phase abundance/%	a/nm	b/nm	c/nm	V/nm^3
As-cast	C15	76.48	0.704 78	–	–	0.496 60
	C14	15.45	0.499 94		0.815 65	0.176 55
	Zr_7M_{10}	8.07	1.232 03	0.920 41	0.920 41	
Melt-spun	C15	69.43	0.704 64	–	–	0.496 52
	C14	30.57	0.497 82	–	0.813 75	0.174 65

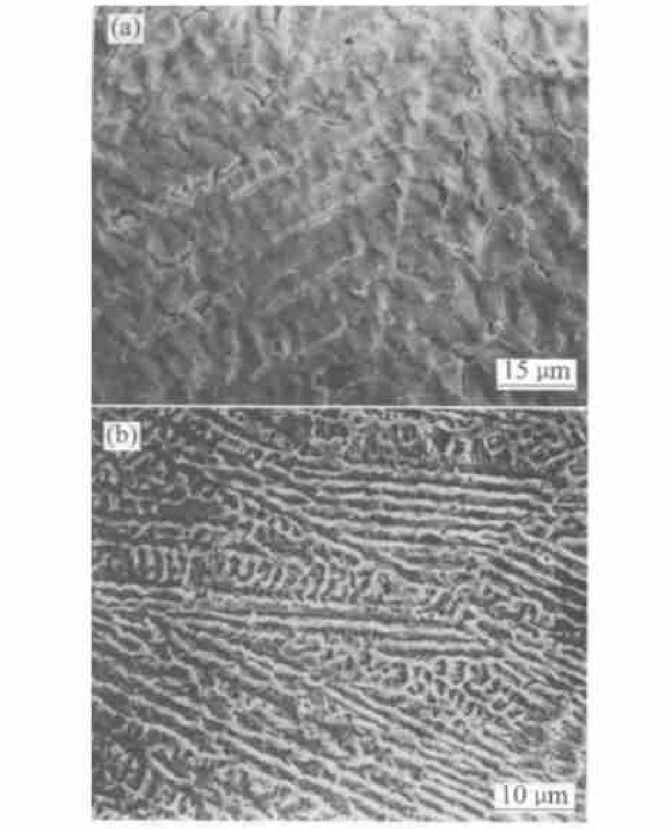

Fig. 4 SEM morphologies of $Zr(MnVNi)_{2.4}$ alloys
(a) —As-cast; (b) —Melt-spun

Fig. 5 shows the discharge curves of the as-cast alloy and melt-spun alloys $Zr(Mn_{0.2}V_{0.2}Ni_{0.6})_{2.4}$ at a discharge rate of 50 mA·hg^{-1}. The discharge curve of the melt-spun alloy is flatter than that of the as-cast alloy, however, the discharge potential of the melt-spun alloy is lower than that of the arc-melted alloy. Generally, the discharge potential flat characteristics are decided by the homogeneity of the alloy composition. The more homogeneous the alloy , the flatter the discharge potential plateau. This result indicates that the melt-spinning process enhances the compositional homogeneity of the alloy.

Fig. 6 shows the activation processes of the two alloys $Zr(Mn_{0.2}V_{0.2}Ni_{0.6})_{2.4}$. It can be seen that the as-cast alloy is activated much easier than the melt-spun alloy. The melt-spun alloy needs 25 charge-discharge cycles to get its highest capacity, but the as-cast alloy only needs 13 cycles. The maximum discharge capacity of melt-spun alloy is 347.5 mA·hg^{-1}, which is a little higher than that of as-cast alloy whose maximum capacity is 340.8 mA·hg^{-1}.

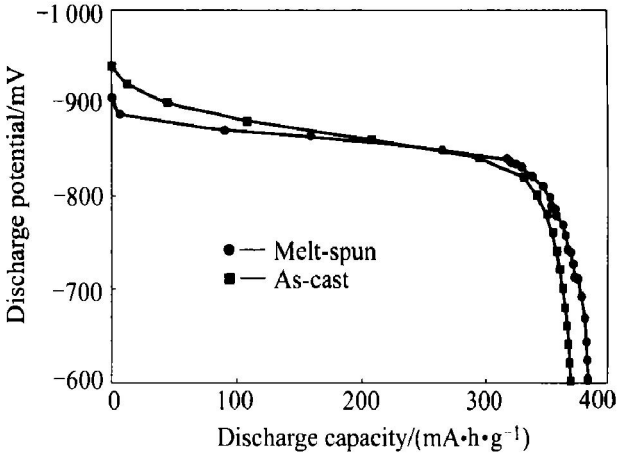

Fig. 5 Discharge curves of as-cast and melt-spun $Zr(MnVNi)_{2.4}$ alloys

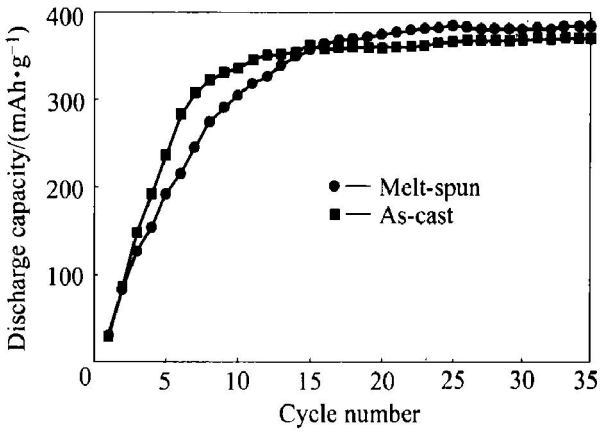

Fig. 6 Activation process of $Zr(Mn_{0.2}V_{0.2}Ni_{0.6})_{2.4}$ alloys

Fig. 7 shows the electrochemical cycling stability of the two alloys $Zr(Mn_{0.2}V_{0.2}Ni_{0.6})_{2.4}$. The results indicate that the cycling stability of melt-spun alloy is much better than that of the as-cast alloy. After 500 charge-discharge cycles, the capacity attenuation rate of the melt-spun alloy is 90.8%, and that of

the as-cast alloy is 80.9%. Table 2 shows the total electrochemical properties of the two alloys. From Table 2 it can be seen that the high-rate-dischargeability of the as-cast alloy is better than that of the melt-spun alloy. The reasons why the two alloys have different electrochemical properties are are analyzed below.

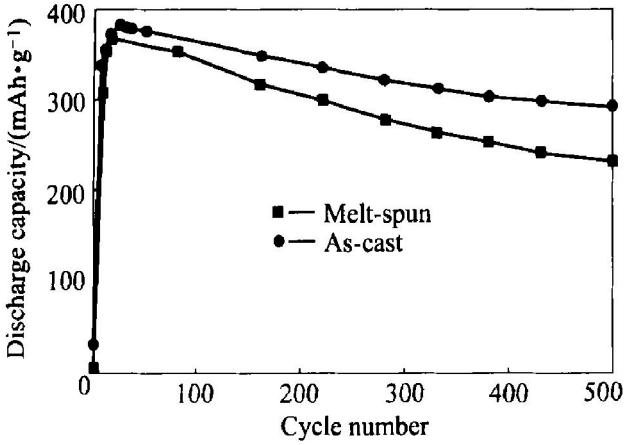

Fig. 7 Cycling stability property curves of $Zr_{0.7}Ti_{0.3}(MnVNi)_{2.4}$ alloys

Table 2 Electrochemical properties of $Zr(Mn_{0.2}V_{0.2}Ni_{0.6})_{2.4}$ alloys

Alloy	Discharge capacity/ ($mAh \cdot g^{-1}$)	Cycling stability/% (c_{500}/c_{max})
As-cast	340.8	80.9
Melt-spun	347.5	90.8

Alloy	High-rate dischargeabiblity at different discharge current/% ($c_n/(c_n+c_{50})$)		
	$N=300$	$N=450$	$N=600$
As-cast	77.9	50.2	42.5
Melt-spun	57.6	40.3	36.8

Firstly, the two alloys have two kinds of phase composition. The as-cast alloy has non-Laves phase Zr_7M_{10} besides C14 and C15 Laves phase, meanwhile the melt-spun alloy only has C14 and C15 Laves phase. It is well known that non-Laves phase Zr_7M_{10} has good electrochemical catalytic property although its charge-discharge capacity is very low (about 100 $mAh \cdot g$). And the phase abundance of C15 phase is different. The C15 phase abundance increases after rapid solidification process. The C14 phase and C15 phase have different electrochemical properties.

Secondly, the two alloys have different microstructure. The grain size of the melt-spun alloy is much smaller than that of the as-cast alloy, in charge-discharge cycles, the hydrogen atoms in the bulk of the electrode can result in lattice strain, and the fine microstructure makes the bulk flexible and release the lattice strain much easier, and suppresses the pulverization in the charge-discharge cycles, thus the activation process is rationally hindered, and the cycling stability improved. In addition, the rapid solidification process eliminate the segregation of elements effectively[7], thus improving the oxidation resistance and the cycling stability of the alloy.

REFERENCES

[1] Notten P H L, Einerhand R E F, Daams J L C. Non-stoichiometric hydride-forming compounds: An excellent combination of long-term stability and high electrocatalytic activity [J]. Z für Phys Chem, Bd, 1994, 183: 267.

[2] Notten P H L, Einerhand R E F, Daams J L C. On the nature of the electrochemical cycling stability of non-soichiometric $LaNi_5$-based hydride-forming compounds Part Ⅰ. Crystallography and electrochemistry [J]. J Alloys Comps, 1994, 210: 221.

[3] Iwakura C, Miyamoto M, Inoue H, et al. Electrochemical evaluation of thermodynamic parameters for dissolved hydrogen in stoichiometric and nonstoichiometric hydrogen storage alloys [J]. J Alloys Comps, 1997, 259: 129.

[4] Iwakura C, Miyamoto M, Inoue H, et al. Effect of stoichiometric ratio on discharge efficiency of hydrogen storage alloy electrodes [J]. J Alloys Comps, 1997, 259: 132.

[5] ZHANG Shu-kai, LEI Yong-quan, CHEN Li-xin, et al. Electrode characteristics of non-stoichiometric $Ml(NiMnAlFe)_x$ alloys [J]. Trans Nonferrous Met Soc China, 2001, 11(2): 183.

[6] GAO Xue-ping, SONG De-ying, ZHANG Yun-shi, et al. Characteristic of the stoichiometric and non-stoichiometric Laves phase alloys and their hydride electrode [J]. J Alloys Comps, 1995, 223: 77.

[7] Lee S M, Lee H, Kim J H, et al. A study on the development of the hypo-stoichiometric Zr-based hydrogen storage alloys with ultra-high capacity for anode material of Ni/MH secondary battery [J]. J Alloys Comps, 2000, 308: 259.

[8] LI Chuan-Jian, WANG Xin-Lin. The relations between microstructure and the capacity decay rate of $MLNi_{3.8}Co_{0.6}Mn_{0.55}Ti_{0.05}$ alloy — (Ⅰ). Capacity decay rate measurements [J]. J Alloys and Comps, 1998, 270: 242.

[9] TANG Wei-zhong, SUN Guang-fei. Electrode stability of La-Ni-Mn hydride-forming materials prepared by conventional and rapid quenching techniques [J]. J Less-Common Met, 1994, 203: 195.

[10] LEI Y Q, ZHANG S K, LÜ G L, et al. Influence of the material processing on the electrochemical properties of cobalt-free $Ml(NiMnAlFe)_5$ alloy [J]. J Alloys and Comps, 2002, 330-332: 861.

[11] ZHANG S K, WANG Q D, LEI Y Q, et al. The phase structure and electrochemical properties of the melt-spun alloy [J]. J Alloys and Comps, 2002, 330-332: 855.

[12] Higashiyama N, Matsuura Y, Nakamura H, et al. Influence of preparation methods of non-stoichiometric hydrogen-absorbing alloys on the performance of nickel-metal hydride secondary batteries [J]. J Alloys Comps, 1997, 253-254: 648.

(Edited by LONG Huai-zhong)